4692 *J. Am. Chem. Soc.* **2000,** *122,* 4692−4699

Gas-Phase Conformations of Synthetic Polymers: Poly(ethylene glycol), Poly(propylene glycol), and Poly(tetramethylene glycol)

Jennifer Gidden,[†] Thomas Wyttenbach,[†] Anthony T. Jackson,[‡] James H. Scrivens,[‡] and Michael T. Bowers*[,†]

*Contribution from the Department of Chemistry, University of California,
Santa Barbara, California 93106, and ICI Research and Technology Centre,
Wilton, Middlesbrough, Cleveland TS 90 8JE, UK*

Received August 25, 1999. Revised Manuscript Received March 6, 2000

Abstract: Effects of chain flexibility and cationizing agent on the gas-phase conformations of a series of polyethers were studied. Collision cross-sections of poly(propylene glycol) (PPG) and poly(tetramethylene glycol) (PTMEG) oligomers (from the 5-mer to 14-mer) cationized by sodium were measured using ion mobility methods and compared to earlier work on sodiated poly(ethylene glycol) (PEG). Molecular mechanics/dynamics calculations show that all three polyethers form a ring of oxygen atoms around Na^+, coordinating additional oxygens to the cation from above and/or below this ring. However, the number and arrangement of these oxygens are system dependent. Up to 8 oxygens in PEG coordinate Na^+, but that number drops to 7 for PPG and 6 for PTMEG. The difference is attributed to changes in the structural details of the ring as well as the position of the Na^+ ion in that ring. Molecular mechanics/dynamics calculations were also used to investigate the structures of neutral PPG and PTMEG oligomers. In these cases, the oligomers are relatively compact below 200 K but they suddenly unfold into more extended structures between 200 and 300 K.

Introduction

Synthetic polymers are often chosen for particular applications based on whether their physical properties, such as glass transition temperatures, stress/strain limitations, or radiative and oxidative stability, meet the required design and processing demands. One characteristic these properties have in common is that they are all known to vary widely with the composition and flexibility of the polymer chain.[1] Consequently, there is great interest in probing the structure of synthetic polymers to determine its role in influencing these properties.

Various analytical methods are available for the characterization of polymer structure. Chromatographic techniques and IR and NMR spectroscopy are some of the more popular choices. However, these methods generally require the polymer to be in solution and the results can often be solvent dependent. One method that is gaining popularity for investigating the gas-phase structures of polymers is mass spectrometry. This technique has long been used to determine fundamental energetic and structural properties of small organic molecules, but the development of electrospray ionization (ESI)[2] and matrix assisted laser desorption/ionization (MALDI)[3] sources has made it possible to obtain similar information on large macromolecules as well.

Much of the research in the mass spectrometry of polymers focuses on measuring molecular weight distributions,[4−8] identifying end groups,[9−11] or determining the sequence and composition of copolymers.[12−14] These studies provide valuable information on the primary and secondary structures of polymers, but they do not give the same level of information on the tertiary structures, or conformations. Numerous studies on biological polymers have shown that conformation can have a tremendous impact on observed properties.[15] However, only recently has much interest been shown in the gas-phase conformations of synthetic polymers, despite the fact they are often simpler systems to model. Proteins and polynucleotides are usually quite complex molecules comprised of many different subunits with different structures and chemical properties. Synthetic homopolymers, on the other hand, are simply long chains with the same repeating unit and therefore may be able to provide insight into folding characteristics and interactions of macromolecules that biopolymers cannot.

[†] University of California.

[‡] ICI Research and Technology Centre.

(1) Fried, J. R. *Polymer Science and Technology*; Prentice Hall: Upper Saddle River, NJ, 1995.

(2) Fenn, J. B.; Mann, N.; Weng, C. K.; Wong, S. F. *Mass Spectrom. Rev.* **1990**, *9*, 37.

(3) Hillenkamp, F.; Karas, M.; Beavis, R. C.; Chait B. T. *Anal. Chem.* **1991**, *63*, 1193A.

(4) Bahr, U.; Deppe, A.; Karas, M.; Hillenkamp, F. *Anal. Chem.* **1992**, *64*, 2866.

(5) Dey, M.; Castoro, J. A.; Wilkins, C. L. *Anal. Chem.* **1995**, *67*, 1575.

(6) Montaudo, G.; Montaudo, M. S.; Puglisi, C.; Samperi, F. *Macromolecules* **1995**, *28*, 4562.

(7) O'Connor, P. B.; McLafferty, F. W. *J. Am. Chem. Soc.* **1995**, *117*, 12826.

(8) Chaudhary, A. K.; Critchley, G.; Diaf, A.; Beckmann, E. J.; Russell, A. J. *Macromolecules* **1996**, *29*, 2213.

(9) de Koster, C. G.; Duursma, M. C.; van Rooij, G. J.; Heeren, R. M. A.; Boon, J. J. *Rapid Commun. Mass Spectrom.***1995**, *9*, 957.

(10) Jackson, A. T.; Yates, H. T.; Scrivens, J. H.; Critchley, G.; Brown, J.; Green, M. R.; Bateman, R. H. *Rapid Commun. Mass Spectrom.* **1996**, *11*, 1668.

(11) Weidner, St.; Kuhn, G. *Rapid Commun. Mass Spectrom.* **1996**, *10*, 942.

(12) Nuwaysir, L. M.; Wilkins, C. L.; Simonsick, W. J., Jr. *J. Am. Soc. Mass Spectrom.* **1990**, *1*, 66.

(13) van Rooij, G. J.; Duursma, M. C.; de Koster, C. G.; Heeren, R. M. A.; Boon, J. J.; Schuyl, P. J.; van der Hage, E. R. E. *Anal. Chem.* **1998**, *70*, 843.

(14) Wilczek-Vera, G.; Yu, Y.; Waddell, K.; Danis, P. O.; Eisenberg, A. *Rapid Commun. Mass Spectrom.* **1999**, *13*, 764.

(15) Creighton, T. E. *Proteins: Structures and Molecular Properties*; Freeman: New York, 1993.

10.1021/ja993096+ CCC: $19.00

To obtain gas-phase conformational data on synthetic polymers (and other macromolecules), we have combined mass spectrometry with an ion mobility based "ion chromatography" (IC) method.[16] IC is based on the principle that ions with different conformations have different collision cross-sections and, consequently, will have different mobilities when drifting through a buffer gas under the influence of a weak electric field. Theoretical methods are then used to generate candidate structures of the ions and calculate their corresponding mobilities for comparison to experiment. This method has been successfully used to accurately measure conformational details of a variety of macromolecules including carbon clusters,[17] crown ethers,[18] biopolymers,[19−22] and synthetic polymers.[23−25]

One particular polymer that has been studied with our IC method is poly(ethylene glycol) (PEG) cationized by a variety of alkali cations.[18b,23] It was found that the PEG oligomers enveloped the metal ion (coordinating up to 11 oxygen atoms for Cs$^+$), forming ball-like structures. A question that arose from these studies was how would the metal ion's influence on conformation change as the composition and flexibility of the polyether changed. Therefore, we turned our attention to poly(propylene glycol) (PPG) and poly(tetramethylene glycol) (PTMEG).

PEG: $HO\!\left(CH_2CH_2O\right)_n\!H$

PPG:

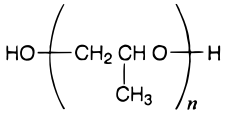

$HO\!\left(CH_2CH(CH_3)O\right)_n\!H$

PTMEG: $HO\!\left(CH_2CH_2CH_2CH_2O\right)_n\!H$

In this paper, we will discuss our recent results concerning the gas-phase conformations of PPG and PTMEG oligomers cationized by sodium ions and compare them to the previous results on sodiated PEG. These polyethers often find commercial uses as lubricants or surfactants but they have also sparked interest in their potential as polymer electrolytes for use in batteries or fuel cells. In these cases, the oligomer's ability to function properly depends on how well it can coordinate alkali cations,[26] so our focus here will be on investigating the nature of the cation−polyether interaction and determining how the flexibility (and thus conformation) of the polyether affects that interaction.

Experimental Section

Sodiated PPG and PTMEG ions (Na$^+$PPG and Na$^+$PTMEG) were produced in a specially designed MALDI ion source.[23b] 2,5-Dihydroxybenzoic acid was used as the matrix and a 50/50 mixture of water and methanol as solvent. Approximately 100 μL of a 1:500 mixture of oligomer and matrix doped with NaI was applied to the sample target and dried. Once ions are formed they are accelerated to 5 kV and mass selected with a reverse geometry, magnetic/electric sector mass spectrometer. The selected ions are then decelerated to 5−10 eV and injected in 1−5 μs pulses into a temperature-variable drift cell[26] containing $\sim$3 Torr of He gas. The ions drift through the gas under the influence of a weak electric field (5−25 V/cm), pass through a quadrupole mass filter, and are detected using standard ion counting techniques.

The drift time of the ions through the cell is measured to give an arrival time distribution (ATD). The mobility, K, of the ions may be determined from this drift time using eq 1,[28] where t_d is the drift time,

$$K = \frac{z}{t_d E} \tag{1}$$

z is the cell length (4 cm), and E is the electric field strength. Using kinetic theory, the mobility, in turn, can be expressed in terms of a collision integral $\Omega^{(1,1)}$[28] that contains information about the ion's shape

$$K = \frac{C}{\Omega^{(1,1)} T^{1/2}} \tag{2}$$

where C is a constant that includes known data about the pressure and mass of the buffer gas as well as the charge and mass of the ion and T is temperature. In short, these two equations show that a longer drift time corresponds to a lower mobility and a larger collision integral.

Because of the size of the oligomers, and their ability to undergo numerous conformational changes due to low rotational barriers, molecular mechanics/dynamics methods were required to generate candidate structures for comparison with experiment. We used the AMBER 4.0 parametrizations[29] which have been shown to yield low-energy structures that correlate with experiment in many previous studies.[18,19,23−25] A series of annealings and energy minimizations[19a,25b] produced 100−150 low-energy structures for each oligomer. Unfortunately, $\Omega^{(1,1)}$ is too difficult to calculate rigorously for these structures (and hence be compared to experiment) but it has been shown that a modified hard-sphere collision cross-section may be used as an acceptable substitute.[17−19,23−25,30−32] These collision cross-sections are calculated for each theoretical structure (averaged over hundreds of random orientations) using previously developed Monte Carlo algorithms.[16] A scatter plot of cross-section vs energy is then created to aid in the structural identification of the oligomer ions measured by the IC experiments.

Results/Discussion

1. Na. Mass spectra of sodiated PPG (M_w = 780) and PTMEG (M_w = 1000) obtained at an off-axis detector before

---

(16) (a) Kemper, P. R.; Bowers, M. T. *J. Phys. Chem.* **1991**, *95*, 5134. (b) Bowers, M. T.; Kemper, P. R.; von Helden, G.; van Koppen. P. A. M. *Science* **1993**, *260*, 1446.

(17) (a) von Helden, G.; Hsu, M.-T.; Kemper, P. R.; Bowers, M. T. *J. Chem. Phys.* **1991**, *95*, 3835. (b) von Helden, G.; Kemper, P. R.; Gotts, N. G.; Bowers, M. T. *Science* **1993**, *249*, 1300. (c) von Helden, G.; Hsu, M.-T.; Gotts, N. G.; Bowers, M. T. *J. Phys. Chem.* **1993**, *97*, 8182. (d) Gotts, N. G.; von Helden, G.; Bowers, M. T. *Int. J. Mass Spectrom. Ion Process.* **1995**, *149/150*, 217.

(18) (a) Lee, S.; Wyttenbach, T.; von Helden, G.; Bowers, M. T. *J. Am. Chem. Soc.* **1995**, *117*, 10159. (b) Wyttenbach, T.; von Helden, G.; Bowers, M. T. *Int. J. Mass Spectrom. Ion Process.* **1997**, *165/166*, 377.

(19) (a) Wyttenbach, T.; von Helden, G.; Bowers, M. T. *J. Am. Chem. Soc.* **1996**, *118*, 8355. (b) Lee, S.; Wyttenbach, T.; Bowers, M. T. *Int. J. Mass Spectrom. Ion Process.* **1997**, *167/168*, 605. (c) Wyttenbach, T.; Bushnell, J. E.; Bowers, M. T. *J. Am. Chem. Soc.* **1998**, *120*, 5098.

(20) Clemmer, D. E.; Hudgins, R. R.; Jarrold, M. F. *J. Am. Chem. Soc.* **1995**, *117*, 10141.

(21) Shelimov, K.; Jarrold, M. F. *J. Am. Chem. Soc.* **1996**, *118*, 10313.

(22) Clemmer, D. E.; Jarrold, M. F. *J. Mass Spectrom.* **1997**, *32*, 577.

(23) (a) von Helden, G.; Wyttenbach, T.; Bowers, M. T. *Science* **1995**, *267*, 1483. (b) von Helden, G.; Wyttenbach, T.; Bowers, M. T. *Int. J. Mass Spectrom. Ion Process.* **1995**, *146/147*, 349.

(24) Gidden, J.; Jackson, A. T.; Scrivens, J. H.; Bowers, M. T. *Int. J. Mass Spectrom. Ion Process.* **1999**, *188*, 121.

(25) (a) Gidden, J.; Wyttenbach, T.; Batka, J. J., Jr.; Weis, P.; Jackson, A. T.; Scrivens, J. H.; Bowers, M. T. *J. Am. Chem. Soc.* **1999**, *121*, 1421. (b) *J. Am. Soc. Mass Spectrom.* **1999**, *10*, 883.

(26) Ratner, M. A.; Shriver, D. F. *Chem. Rev.* **1988**, *88*, 109.

(27) Kemper, P. R.; Bowers, M. T. *J. Am. Soc. Mass Spectrom.* **1990**, *1*, 197.

(28) Mason, E. A.; McDaniel, E. W. *Transport Properties of Ions in Gases*; Wiley: New York, 1988.

(29) Pearlman, D. A.; Case, D. A.; Caldwell, J.; Seibel, G. L.; Singh, U. C.; Weiner, P.; Kollman, P. A. *AMBER 4.0*, University of California, San Francisco, CA, 1991.

(30) Wyttenbach, T.; von Helden, G.; Batka, J. J., Jr.; Carlat, D.; Bowers, M. T. *J. Am. Soc. Mass Spectrom.* **1997**, *8*, 275.

(31) Mesleh, M. F.; Hunter, J. M.; Shvartsburg, A. A.; Schatz, G. C.; Jarrold, M. F. *J. Phys. Chem.* **1996**, *100*, 16082.

(32) Shvartsburg, A. A.; Schatz, G. C.; Jarrold, M. F. *J. Chem. Phys.* **1998**, *108*, 2416.

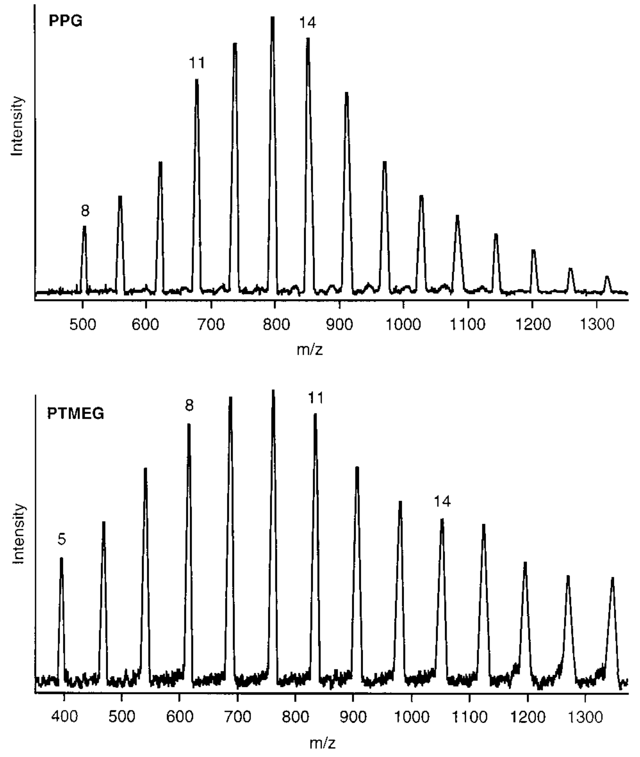

Figure 1. MALDI mass spectra of PPG ($M_w = 780$) and PTMEG ($M_w = 1000$) cationized by Na^+. Na^+PPG and Na^+PTMEG ions selected for theoretical analyses are labeled by their number of repeat units.

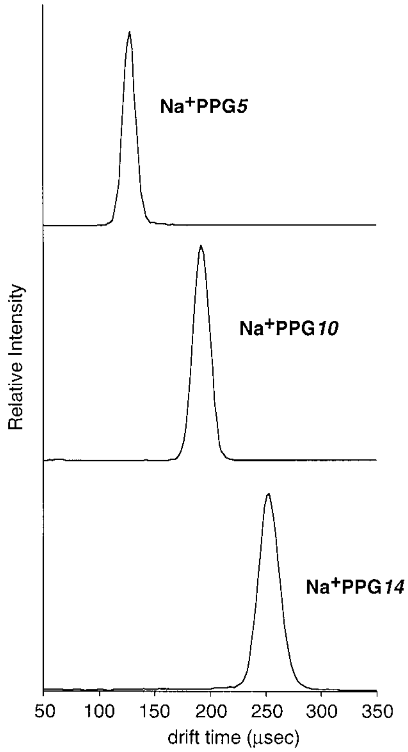

Figure 2. Typical ATDs for Na^+PPG*5*, Na^+PPG*10*, and Na^+PPG*14* at 300 K. A single peak is observed for all oligomers at all temperatures studied. The average drift time increases with oligomer size, consistent with an increase in cross-section.

the drift cell are given in Figure 1. Na^+PPG and Na^+PTMEG ions selected for theoretical analyses are labeled with their number of repeat units. Ion chromatography (IC) experiments were performed on Na^+PPG*5* to Na^+PPG*15* (i.e. from the 5-mer to the 15-mer) and on Na^+PTMEG*5* to Na^+PTMEG*12*. A second PPG sample ($M_w = 400$) was used to obtain data on Na^+PPG*5* to Na^+PPG*7*. Although the intensities of the largest *m*/*z* ions are similar to those in the lowest *m*/*z* range, the larger ions are more difficult to inject into the drift cell. As a result, experimental data were limited to the 15-mer for PPG and the 12-mer for PTMEG.

Typical arrival time distributions (ATDs) obtained from the IC experiments are shown in Figure 2 for Na^+PPG*5*, Na^+PPG*10*, and Na^+PPG*14* at a cell temperature of 300 K. One expected feature shown in the ATDs is that the average drift time increases with oligomer size, thus indicating an increase in cross-section. Also apparent in the ATDs is the sole presence of single, symmetric peaks. This was observed in the ATDs of all oligomers (including PEG and PTMEG) at all temperatures (100−570 K). Single peaks in ATDs usually indicate that either one isomer exists or if multiple isomers are present they either have very similar cross-sections or rapidly interconvert on the time scale of the experiment. Prior studies on carbon clusters[17] and PET oligomers[25] showed that isomers with cross-sections differing as little as 5−10% clearly appear as shoulders or distinct, separate peaks in the ATDs.

From these ATDs, the mobilities and cross-sections of the ions may be determined. A plot of cross-section vs chain length is shown in Figure 3a for Na^+PEG, Na^+PPG, and Na^+PTMEG ions. The cross-sections of all three polyethers increase almost linearly with oligomer size, which is common for ions that are structurally related.[17,23,24] The plot also shows that the "slopes" of the three lines are different. The cross-section of Na^+PTMEG increases faster per added repeat unit than Na^+PPG, which increases faster than Na^+PEG. This is due to the fact that each TMEG unit adds another 13 atoms, while each PG unit adds just 10 atoms, and each EG unit only 7 atoms. When all data are plotted as a function of the number of atoms (Figure 3b) a single slope is obtained.

Figure 3 also shows the cross-sections obtained from the lowest energy theoretical structures (open circles). At least 100 structures were calculated for a given oligomer and their cross-sections determined by the protocols referred to in the Experiment Section. A scatter plot of cross-section vs energy is then generated for structural analyses. An example of such a plot is given in Figure 4 for Na^+PTMEG*8*. This example points out a trend observed in the scatter plots of all the oligomers: the most stable structures are the most compact while the unfolded, larger cross-section structures are higher in energy. The average cross-sections of the lowest 2−5 kcal/mol structures (which are very similar to each other with only minor variations in geometry) are used in the comparison to experiment in Figure 3. Deviations between the experimental and theoretical cross-sections for all compared oligomers in Figure 3 are within ~1%.

Figure 5 shows the lowest energy structures found for Na^+PEG*5*, Na^+PPG*5*, and Na^+PTMEG*5*. They all have two similar features. Each polyether forms a ring of oxygens around Na^+, resembling a crown ether, and all six oxygens in each polyether coordinate to the Na^+ ion. However, the detailed arrangement of those oxygen atoms is different for each polyether. Five oxygens in Na^+PEG*5* form a nearly planar ring around Na^+ while the sixth oxygen bends out of plane to coordinate to the Na^+ ion from above the ring. A similar structure is obtained for Na^+PPG*5* except that the ring of oxygens around the Na^+ ion is not quite as planar as observed for Na^+PEG*5*. In addition, one of the oxygens in the ring has moved slightly out of plane. The CH_3 groups in PPG essentially point away from the Na^+

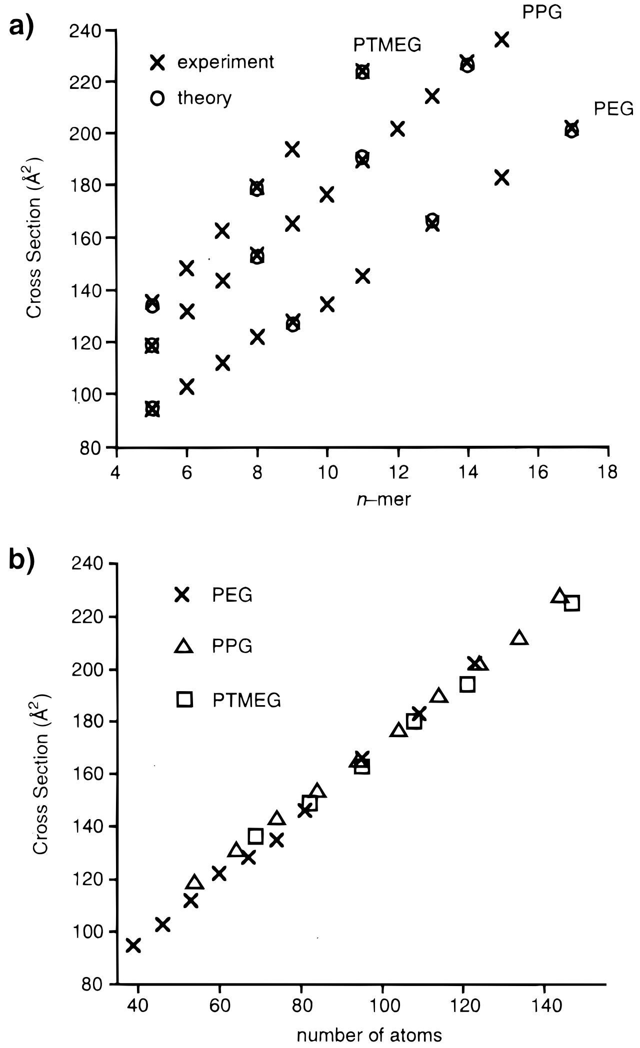

Figure 3. (a) Collision cross-section vs number of repeat units for Na$^+$PEG*n*, Na$^+$PPG*n*, and Na$^+$PTMEG*n* at 300 K. The crosses are from experimental ATDs while the open circles are from the theoretical structures. (b) Experimental cross-section vs number of atoms in the oligomer for the data plotted in part a. Experimental points are crosses for PEG, triangles for PPG, and squares for PTMEG.

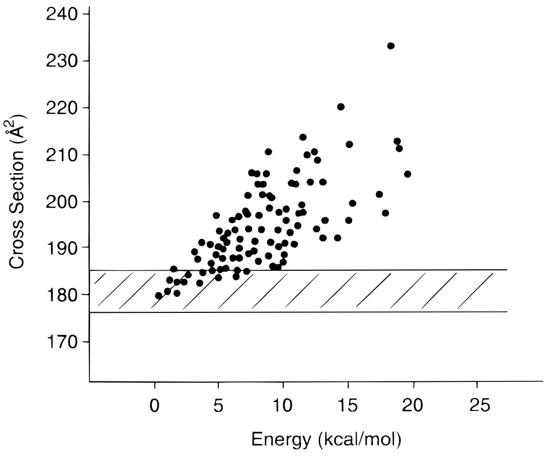

Figure 4. A scatter plot of cross-section vs energy for Na$^+$PTMEG*8*. Each point represents one structure generated by the molecular mechanics/dynamics calculations. The shaded area is the range of experimental cross-sections.

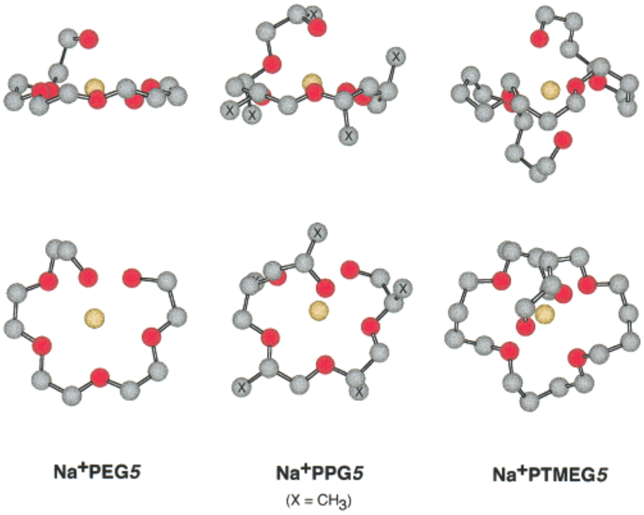

Figure 5. Lowest energy structures of Na$^+$PEG*5*, Na$^+$PPG*5*, and Na$^+$PTMEG*5* (see text). Carbon atoms are shown in gray, oxygen atoms in red, and the Na$^+$ ion in yellow. The methyl group carbons in PPG are distinguished by an X.

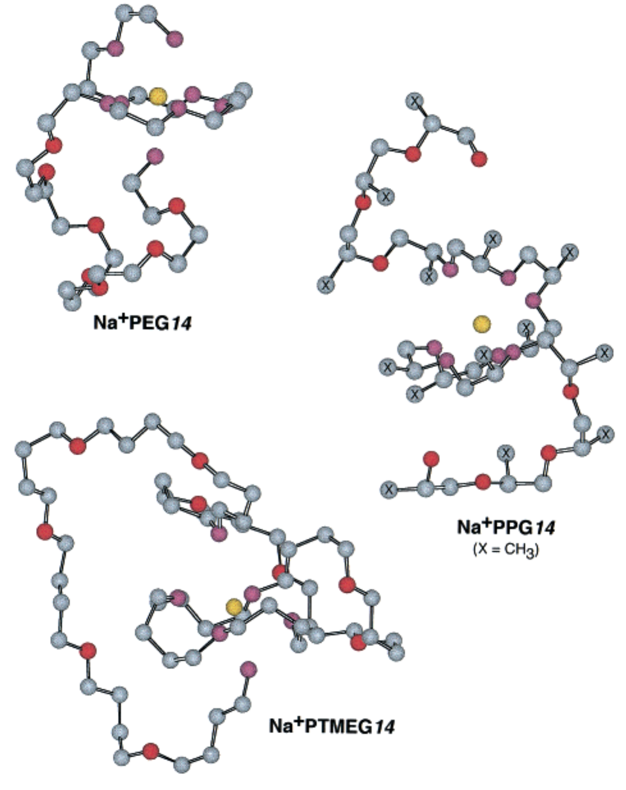

Figure 6. Lowest energy structures for Na$^+$PEG*14*, Na$^+$PPG*14*, and Na$^+$PTMEG*14* (see text). Carbon atoms are shown in gray and oxygen atoms in red. Oxygens <3 Å from the Na$^+$ ion are shown in purple. Hydrogen atoms have been omitted for clarity. The methyl group carbons in PPG are distinguished by an X. Na$^+$PEG*14* has 8 oxygen atoms coordinated to Na$^+$ while Na$^+$PPG*14* has 7, and Na$^+$PTMEG*14* just 6. Note that the arrangement of the oxygens around Na$^+$ is similar to that observed in the corresponding 5-mers (Figure 5).

ion but still create enough of a hindrance to slightly distort the ring and shift the arrangement of the oxygen atoms around the Na$^+$ ion (relative to PEG). The ring of oxygens around Na$^+$PTMEG*5* is even less planar. This polyether has very flexible four-membered carbon chains between oxygen atoms that form loops in the ring around Na$^+$. The longer distance between successive oxygen atoms also limits the number of oxygens in the ring to four and forces the remaining two oxygens to approach the Na$^+$ ion from opposite sides of the ring.

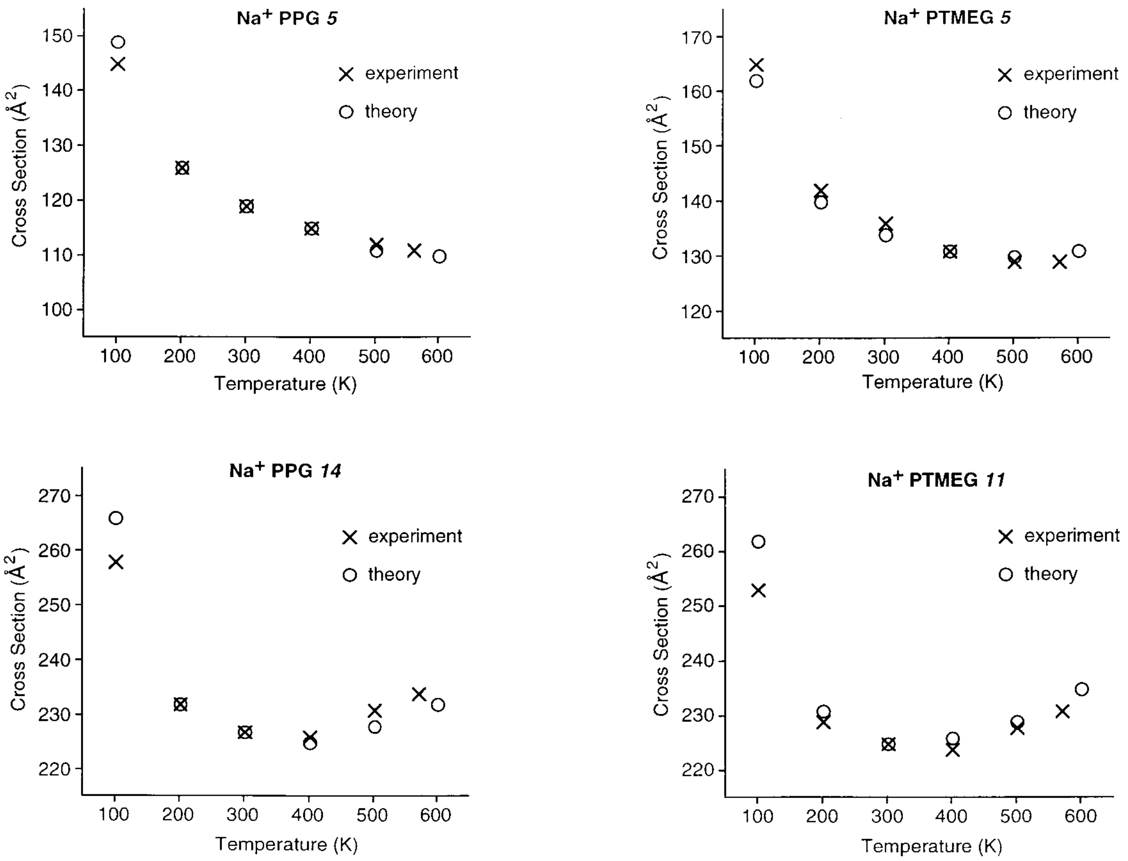

Figure 7. Collision cross-section vs temperature plot for Na$^+$PPG*5*, Na$^+$PPG*14*, Na$^+$PTMEG*5*, and Na$^+$PTMEG*11*. The crosses are experimental data and the open circles are from molecular dynamics simulations (see text and Figure 8).

These basic structural features found in the 5-mers are also present in the larger oligomers. This can be seen in the lowest energy structures of Na$^+$PEG*14*, Na$^+$PPG*14*, and Na$^+$PTMEG*14* shown in Figure 6. In each case, the arrangement of the oxygen atoms surrounding the Na$^+$ ion is similar to that observed in the corresponding 5-mer. However, unlike the 5-mer structures, the number of oxygens in the 14-mers that coordinate to Na$^+$ is not the same for each polyether. The Na$^+$ ion coordinates 8 oxygen atoms in Na$^+$PEG*14*, five in a planar ring, two above this ring, and one below it. In Na$^+$PPG*14*, only 7 oxygens coordinate to the Na$^+$ ion. This is most likely a result of the fact that (1) the Na$^+$ ion has moved out of the plane of the ring and (2) the ring of oxygens is bent more than it was in the 5-mer. Consequently, the Na$^+$ ion coordinates to additional oxygen atoms that are above the ring but does not interact with any oxygens that are below the ring (like PEG does). In Na$^+$PTMEG*14*, the number of oxygens coordinating to Na$^+$ remains at 6. The six oxygens are positioned in an octahedral-like arrangement around Na$^+$ and the polyether simply cannot position any more oxygen atoms near the Na$^+$ ion.

To further investigate the role of flexibility on the conformations of these oligomers, we followed their cross-sections as a function of temperature. Figure 7 shows the temperature dependence of the cross-sections of Na$^+$PPG*5*, Na$^+$PPG*14*, Na$^+$PTMEG*5*, and Na$^+$PTMEG*11*. Since the cross-sections scale with $T^{-1/2}$, the plots of all four ions should show a decrease in cross-section with an increase in temperature as seen for Na$^+$PPG*5*. However, the cross-sections of Na$^+$PTMEG*5* remain essentially constant from 400 to 600 K while those of Na$^+$PPG*14* and Na$^+$PTMEG*11* actually increase over this temperature range.

Molecular dynamics simulations can help interpret this unusual cross-section behavior at high temperature. The simulations were begun at a temperature of 200 K and run for 1000 ps. Every picosecond the structure was saved and its cross-section calculated. At the end of the run, the temperature was raised 100 K and the process repeated.

Figure 8 shows the calculated cross-sections of Na$^+$PPG*5*, Na$^+$PPG*14*, Na$^+$PTMEG*5*, and Na$^+$PTMEG*11* as a function of time and temperature. The average cross-sections at each temperature are given as the “theory” points (open circles) in Figure 7. The small spread in cross-section at 200 K is primarily due to the statistical nature of the cross-section calculations (the cross-section of each structure is averaged over many random orientations until a convergence of 1% is reached) and is observed for all ions. As the temperature increases the spread in cross-section increases, but its magnitude differs from system to system.

The calculations on Na$^+$PPG*5* show a maximum variance in cross section of ±5 Å^2 throughout the dynamics run. They also show a slight, steady decrease in average cross-section from 300 to 600 K (119 to 110 Å^2). This matches the trend observed in the experimental results (Figure 7) very well. Na$^+$PPG*14*, on the other hand, has a cross-section spread of ±10 Å^2 at 200 K but that number jumps to ±27 Å^2 at 600 K. Meanwhile, the average cross-section has also increased, from 224 Å^2 at 400 K to 232 Å^2 at 600 K. Again, this trend tracks very nicely with the experimental data.

The differences in cross-section behavior between these two PPG oligomers can be explained by examining their structures. In Na$^+$PPG*5*, every oxygen atom in the oligomer is strongly coordinated to the Na$^+$ ion. During the entire dynamics run,

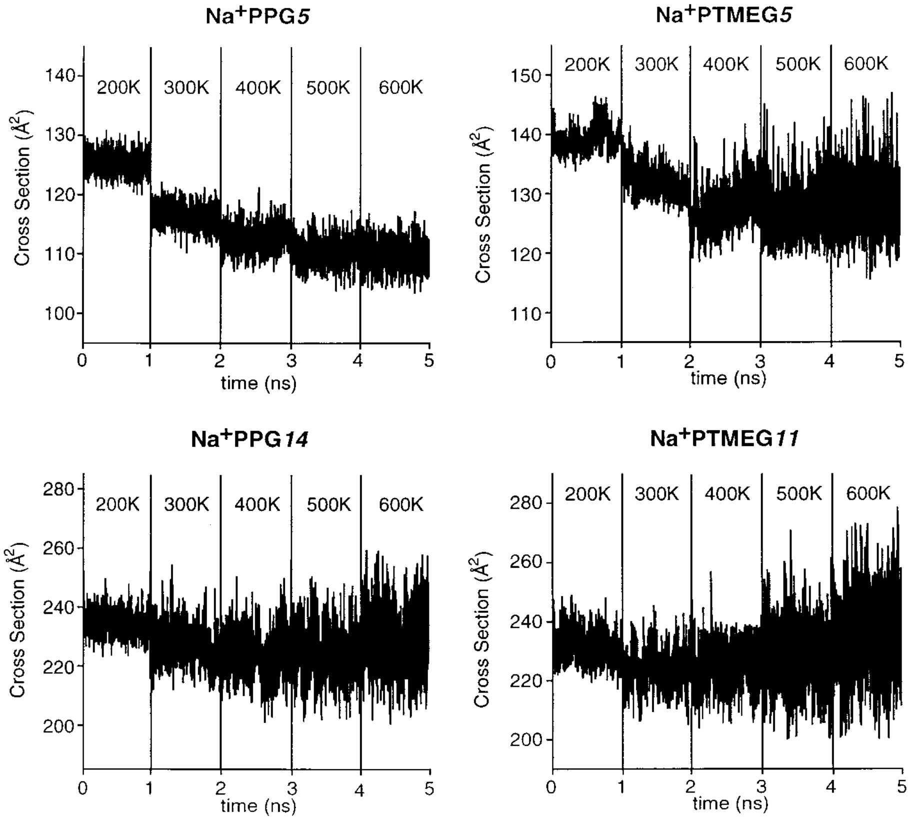

Figure 8. Theoretical cross-section vs time and temperature plot for the lowest energy structures of Na$^+$PPG*5*, Na$^+$PPG*14*, Na$^+$PTMEG*5*, and Na$^+$PTMEG*11* determined from molecular dynamics simulations (see text). The average cross-sections at each temperature are shown as the open circles in Figure 7. The small spread in cross-section at low temperatures is due to statistical uncertainty in the calculations (±1%). The deviation in cross-section increases at higher temperatures for all oligomers except Na$^+$PPG*5*. The largest amplitudes in cross-section are observed for Na$^+$-PTMEG*11* with a maximum deviation of ±35 Å^2 at 600 K.

these oxygens remain in contact with the Na$^+$ ion, essentially holding the oligomer in place and not allowing it to significantly expand (at least between 200 and 600 K). In Na$^+$PPG*14*, only 7 of 15 oxygens are coordinated to the Na$^+$ ion. These seven oxygens generally remain coordinated to the Na$^+$ ion throughout the dynamics run (with a few brief exceptions) acting as an anchor for part of the oligomer. However, there is a rather large portion of the oligomer that is remote from the Na$^+$ ion that begins to unravel at higher temperatures thus increasing the average "size" (or cross-section) of the oligomer.

The plots for Na$^+$PTMEG*5* and Na$^+$PTMEG*11* are similar to those of the Na$^+$PPG oligomers in that the larger oligomers expand more at higher temperatures. However, there are some differences when directly comparing similar sized PTMEG and PPG oligomers. For example, the maximum variance in cross-section at 600 K for Na$^+$PTMEG*5* is twice that of Na$^+$PPG*5* (±10 to ±5 Å^2). In addition, the average cross-section of Na$^+$PTMEG*5* essentially remains constant at ~132 Å^2 from 300 to 600 K, whereas the average cross-section for Na$^+$PPG*5* slightly decreases over this temperature range. These results indicate that Na$^+$PTMEG*5* undergoes greater molecular motion than Na$^+$PPG*5* even though both oligomers have all six oxygens coordinated to Na$^+$. An analogous comparison can be made between Na$^+$PTMEG*11* and Na$^+$PPG*14*. Both oligomers have the same number of atoms and a similar percentage of total oxygens coordinated to Na$^+$ (6 of 12 for Na$^+$PTMEG*11* and 7 of 15 for Na$^+$PPG*14*), but the maximum spread in cross-section at 600 K is 70 Å^2 for Na$^+$PTMEG and just 55 Å^2 for Na$^+$PPG*14*. These differences can be attributed not only to the nature of the Na$^+$–O interaction but also to the structures of the oligomer chains themselves. PTMEG has a very flexible backbone and forms rather "floppy" molecules (see Figures 5 and 6). As a result, Na$^+$PTMEG oligomers are capable of large-scale molecular motion at relatively low temperatures. Even the ring of oxygens around Na$^+$ has significant movement during the dynamics simulations. Na$^+$PPG, on the other hand, is hindered in its motion by the CH_3 side groups. The ring of oxygens around Na$^+$, although bent, remains relatively rigid throughout the dynamics run and the portions of the oligomer remote from the Na$^+$ ion do not appear to have the same freedom of movement as those in the Na$^+$PTMEG oligomers.

2. Neutral Oligomers. Molecular mechanics/dynamics calculations were also run for neutral PPG and PTMEG (from the 5- to 14-mer) to determine how the oligomers prefer to fold in the absence of metal cation. IC experiments cannot be performed on neutral species, so there are no experimental data to check the validity of these theoretical structures. However, the excellent agreement between experimental and theoretical cross-sections obtained for the alkalated species, not only in this study but in a number of different polymer systems,[18b,23−25] indicates that the parameters used in the calculations are appropriate. Therefore, the calculations should give reasonable models for the neutral species as well.

Although the two polyethers have different chain structures, they go through similar structural transitions as the oligomer size increases. The smallest oligomers (5- to 8-mer) are quasilinear open structures, but as the oligomers grow they begin to fold, first into U-shaped arrangements (8- to 11-mer) and then into more twisted and compact structures (11- to 14-mer). Examples of the structures are shown in Figure 9 for PTMEG. Calculations on neutral PEG oligomers also showed similar results.

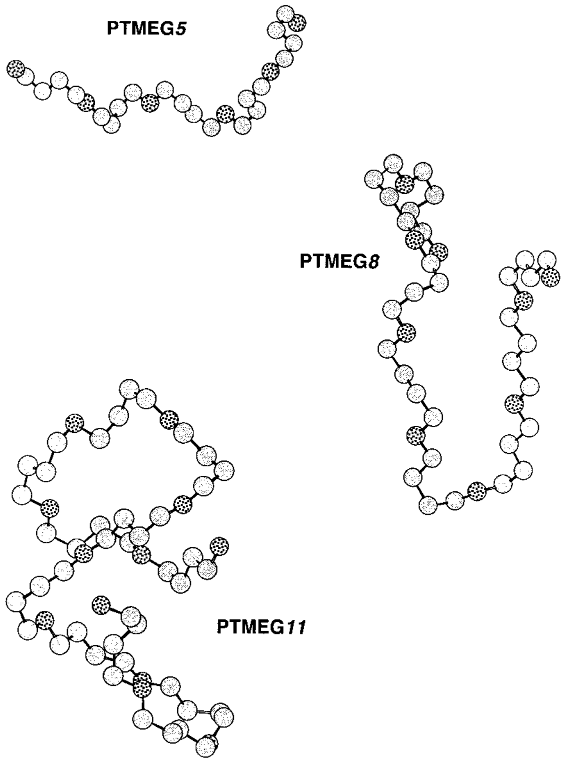

Figure 9. Lowest energy structures found for neutral PTMEG*5*, PTMEG*8*, and PTMEG*11* using molecular mechanics/dynamics calculations. Carbon atoms are gray and oxygen atoms are circles filled with dots. As *n* increases, the oligomer begins to fold on itself, first into a U-shaped arrangement and then into a more twisted and compact structure. Similar structural transitions were observed for neutral PPG and PEG oligomers.

Molecular dynamics simulations were performed on neutral PPG*14* and PTMEG*11*. Cross-section vs time and temperature plots for these oligomers are shown in Figure 10. Each oligomer starts out in its twisted, compact structure but unlike their sodiated counterparts, which gradually expand with temperature, the neutral oligomers open up rather abruptly between 200 and 300 K. In Na^+PPG and Na^+PTMEG, there is a relatively strong electrostatic attraction between the Na^+ ion and the oxygen atoms in the oligomer chains. This effectively keeps the oligomers somewhat compact until a sufficiently high temperature is reached. The major attractive forces present in neutral PPG and PTMEG are relatively weak van der Waals forces and an electrostatic interaction less than half the magnitude of that calculated for the sodiated oligomers. These forces can easily be overcome at low temperatures, thus explaining the sudden unfolding of the neutral oligomers by 300 K.

By the end of the 300 K dynamics, both oligomers have reached their maximum spread in cross-section (±30 Å^2 for PPG*14* and ±43 Å^2 for PTMEG*11*) and maintain a constant average cross-section (~257 Å^2 for PPG*14* and ~284 Å^2 for PTMEG*11*) for the remainder of the simulation. However, PPG*14* takes a little longer time reaching this plateau. Approximately 900 ps into the 200 K dynamics, the average cross-section of PTMEG*11* jumps from 250 to 280 Å^2 and the oligomer is significantly oscillating by the start of the 300 K dynamics. PPG*14* has the same average cross-section from 200 to 600 K and does not reach its maximum variance in cross-section until ~400 ps into the 300 K dynamics. Again, this can be attributed to the flexibility of the oligomer backbones. With CH_3 groups limiting its movement, PPG requires slightly higher temperatures than PTMEG to begin to significantly oscillate.

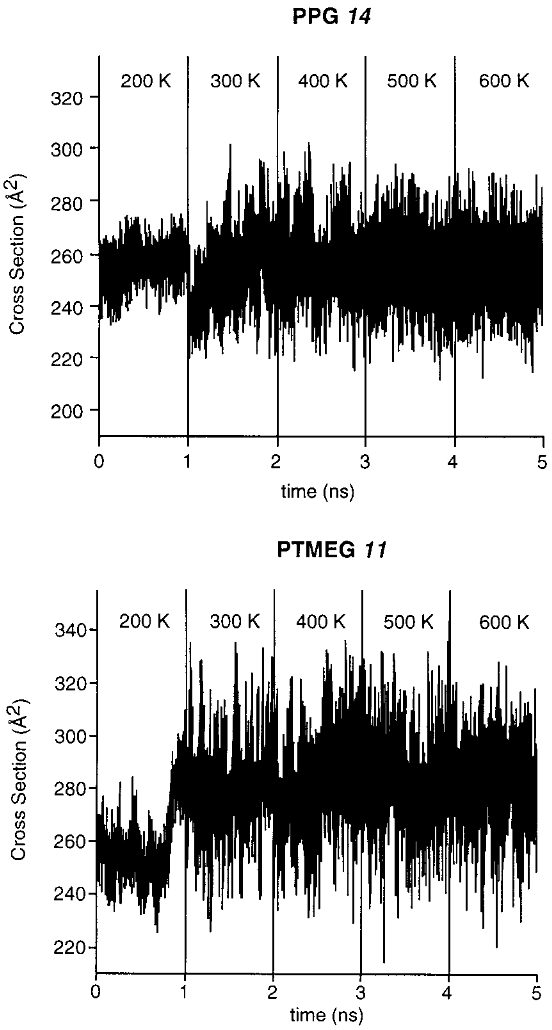

Figure 10. Theoretical cross-section vs time and temperature plots for neutral PPG*14* and PTMEG*11*. Both oligomers start out in relatively compact structures at 200 K with an average spread in cross-section of ±15 Å^2. At 300 K, all motional barriers appear to have been surpassed and the oligomers begin to significantly oscillate. The average cross-section for PTMEG*11* increases from 250 Å^2 to 280 Å^2 about 900 ps into the 200 K dynamics and the average spread in cross-section jumps from ±15 Å^2 to ±35 Å^2. For PPG*14*, the average cross-section spread increases from ±15 Å^2 at 200 K to ±27 Å^2 from 300 to 600 K.

Once the oligomers overcome all motional barriers, they have a rather large spread in cross-section compared to Na^+PPG and Na^+PTMEG. During these fluctuations, the oligomers essentially oscillate between the three structures described in Figure 9. The lowest cross-section structures are low-energy, folded structures and the largest cross-section structures are higher-energy (but entropically favored) linear structures. As the oligomers proceed from one extreme to the other, they pass through U-shaped intermediates.

Conclusion

The combination of ion mobility and molecular mechanics/dynamics calculations can provide valuable insight toward understanding the factors that underlie polymer folding. In the cases of sodiated PEG, PPG, and PTMEG, there exists a competition between the Na^+ ion and the structural details of the oligomer backbone on influencing the overall conformation. While all three polyethers have similar structural features, the simple addition of a methyl group or separation of oxygen atoms can significantly impact the nature of the cation−oligomer interaction. Results of this are seen in the decrease in the number of oxygen atoms coordinated to Na^+ (PEG > PPG > PTMEG) as well as in changes in the dynamics of the folding and unfolding of these oligomers at higher temperatures. Further investigation into the metal cation attachment to these polyethers is underway using Li^+ and Cs^+ as cationizing agents.

Although the influence of charge centers on polymer folding is an important and growing concern, the majority of interest in the conformations of polymers still lies in the neutral species. Ion mobility experiments are not an option in this case but the molecular mechanics/dynamics calculations are. The level of agreement observed between experimental and calculated cross-sections of the sodiated species generates confidence that the theoretical methods used in this work provide very reliable models of the actual oligomers.

Acknowledgment. The support of the Air Force Office of Scientific Research under grants F49620-96-1-0033 and F49620-96-1-0257 and the partial support of the National Science Foundation under grant CHE-9729146 is gratefully acknowledged.

JA993096+